PROCEEDINGS OF SPIE

SPIEDigitalLibrary.org/conference-proceedings-of-spie

Influence of the sensory information complexity on the features of low frequency rhythms of human EEG

Kuc, Alexander, Maksimenko, Vladimir

Alexander Kuc, Vladimir Maksimenko, "Influence of the sensory information complexity on the features of low frequency rhythms of human EEG," Proc. SPIE 11847, Saratov Fall Meeting 2020: Computations and Data Analysis: from Molecular Processes to Brain Functions, 118470R (4 May 2021); doi: 10.1117/12.2591337

SPIE.

Event: Saratov Fall Meeting 2020, 2020, Saratov, Russian Federation

Downloaded From: https://www.spiedigitallibrary.org/conference-proceedings-of-spie on 07 May 2021 Terms of Use: https://www.spiedigitallibrary.org/terms-of-use

Influence of the sensory information complexity on the features of low frequency rhythms of human EEG

Alexander Kuc[1], Vladimir Maksimenko[1,2]

[1]Innopolis University, Universitetskaya St, 1, Innopolis, 420500, Russia;
[2]Saratov State Medical University, Bolshaya Kazachia St., 112, Saratov, 410012, Russia.

ABSTRACT

The perception of visual information includes such stages as the initial processing of sensory input and the interpretation of the received information (decision-making). The uncertainty of visual stimuli affects the neural activity during both sensory-processing and the decision-making stages. Here we analyzed spatial and temporal properties of the neural activity in the β-frequency band during the processing of ambiguous bistable stimuli. We tested how the stimulus ambiguity influenced the perceptual decision-making process.

Keywords: signal analysis, EEG, visual stimuli, ambiguity, perception

1. INTRODUCTION

Analysis of the neural activity during the perception and processing of sensory information is an essential task of computer science and neurophysiology.[1–3] Interest in solving this problem is associated with the possibility of detecting the neural activity features characterizing the perception of a large amount of sensory information in conditions of high cognitive load.[4,5] One of the most effective approaches to analyze the brain neural network is detecting characteristic time-frequency and spatio-temporal features of electrical activity registered by the non-invasive multichannel electroencephalograms (EEG).[6,7]

In this paper, we study the spatio-temporal structure of multichannel EEG signals in the β-frequency band during a cognitive task accomplishment. As a cognitive task, we used the perception of bistable visual stimuli (Necker's cube) and their classification depending on interpretation. This cognitive task includes such processes as a primary perception of visual information and decision-making regarding the interpretation of a visual stimulus.[8] It is known that increasing ambiguity of a visual stimulus affects the response time that the observer takes to interpret visual information and make a decision. In this paper, we studied the effect of the stimulus ambiguity on the brain neural activity in the β-frequency band. We focused on the β-band since the features of neural activity in this band are associated with both the primary processing of visual information[9] and the decision-making process.[10]

2. METHODS

2.1 Experimental procedure

Twenty healthy subjects, between the ages of 26 and 35 with normal or corrected-to-normal visual acuity participated in the experiments. All of them provided informed written consent before participating in the experiment. The experimental studies were performed in accordance with the Declaration of Helsinki and approved by the local research ethics committee of the Innopolis University.

The Necker cube was used as the visual stimuli.[11–13] It represents itself a cube with transparent faces and visible edges; an observer without any perception abnormalities sees the Necker cube as a 3D-object due to the specific position of the cube's edges. Bistability in perception consists in the interpretation of this 3D-object as to be either left- or right-oriented depending on the constrast of different inner edges of the cube. The contrast $a \in [0, 1]$ of the three middle lines centered in the left middle corner was used as a control parameter. The

Further author information: (Send correspondence to A. Kuc)
E-mail: kuc1995@mail.ru , Telephone: +7 927 221 32 93

Saratov Fall Meeting 2020: Computations and Data Analysis: from Molecular Processes to Brain Functions, edited by Dmitry E. Postnov, Proc. of SPIE Vol. 11847, 118470R
© 2021 SPIE · CCC code: 1605-7422/21/$21 · doi: 10.1117/12.2591337

Downloaded From: https://www.spiedigitallibrary.org/conference-proceedings-of-spie on 07 May 2021
Terms of Use: https://www.spiedigitallibrary.org/terms-of-use

values $a = 1$ and $a = 0$ correspond, respectively, to 0 (black) and 255 (white) pixels' luminance of the middle lines. If a is close to 0 or 1, such a Necker cube is easily interpreted as either right-oriented or left-oriented. For $a \sim 0.5$, identifying the orientation of the Necker cube becomes difficult, since such an image has a high level of ambiguity. During the experiment, the subject was randomly shown 400 cubes of Necker with different values of the parameter a.

Participants of the experiment were instructed to press either the left or right key depending on the first impression of the orientation of the Necker cube. Since the perception of the current cube can be influenced by previously demonstrated Necker cubes, the length of the visual stimulus representation varied in the range of $1 - 1.5$ s. Also, a random change in the control parameter a also prevented the stabilization of perception. In addition, abstract images were exhibited for about $\gamma = 3.0 - 5.0$ between demonstrations of the Necker cube image to eliminate the "memory effect".

The EEG signals were recorded using the monopolar registration method and the classical extended ten–ten electrode system. We recorded 31 signals with two reference electrodes A1 and A2 on the earlobes and a ground electrode N just above the forehead. The signals were acquired via the cup adhesive Ag/AgCl electrodes placed on the "Tien–20" paste (Weaver and Company, Colorado, USA). Immediately before the experiments started, we performed all necessary procedures to increase skin conductivity and reduce its resistance using the abrasive "NuPrep" gel (Weaver and Company, Colorado, USA). The impedance was monitored after the electrodes were installed and measured throughout the experiments. Usually, the impedance values varied within a 2–5 kΩ interval. The electroencephalograph "Encephalan-EEG-19/26" (Medicom MTD company, Taganrog, Russian Federation) with multiple EEG channels and a two-button input device (keypad) was used for amplification and analog-to-digital conversion of the EEG signals. The raw EEG signals were filtered by a band-pass filter with cut-off points at 1 Hz (HP) and 100 Hz (LP) and by a 50-Hz notch filter by embedded a hardware-software data acquisition complex.

2.2 Signal analysis

We analyzed the EEG signals power in β-frequency bands, using the continuous wavelet transformation.[14] The wavelet power spectrum $E^n(f,t) = (W^n(f,t))^2$ was calculated for each EEG channel $X_n(t)$ in the frequency range $1 - 30$ Hz. Here, $W^n(f,t)$ is the complex-valued wavelet coefficients calculated as

$$W^n(f,t) = \sqrt{f} \int_{t-4/f}^{t+4/f} X_n(t)\psi^*(f,t)dt, \tag{1}$$

where $n = 1, ..., N$ is the EEG chanel number ($N = 31$ is the total number of chanels used for the analysis) and "*" defines the complex conjugation. The mother wavelet function $\psi(f,t)$ is the Morlet wavelet which is defined as

$$\psi(f,t) = \sqrt{f}\pi^{1/4} \mathrm{e}^{j\omega_0 f(t-t_0)} \mathrm{e}^{f(t-t_0)^2/2}, \tag{2}$$

where $\omega_0 = 2\pi$ is the wavelet parameter.[15]

For β-frequency bands the wavelet amplitudes $E^n_\beta(t)$ were calculated as

$$E^n_\beta(t) = \frac{1}{\Delta f_\beta} \int_{\Delta f_\beta} E^n(f',t)df', \tag{3}$$

where $\Delta f_\beta = 15 - 30$ Hz. The wavelet power of the time-series was calculated for the entire experimental session, and then divided into segments that capture the interval from the presentation of a visual stimulus to the pressing of a button.

Downloaded From: https://www.spiedigitallibrary.org/conference-proceedings-of-spie on 07 May 2021
Terms of Use: https://www.spiedigitallibrary.org/terms-of-use

3. RESULTS

To investigate the effect of visual stimulus complexity, all Necker cubes were divided into two groups (each group included 80 stimuli - 20 for each value of parameter a):

- Low ambiguity (LA) stimuli, including the Necker cube images with $a \in \{0.15, 0.25, 0.75, 0.85\}$
- High ambiguity (HA) stimuli, including the Necker cube images with $a \in \{0.40, 0.45, 0.55, 0.60\}$

We analyzed the changes in the electrical activity of the brain caused by processing visual sensory information. We identified the EEG channels that show a significant increase in the spectral amplitude for seven areas of EEG sensors when processing LA and HA stimuli. Figure 1 shows the distributions of the number of EEG channels N with increasing spectral amplitude. We compared the obtained N values in three time intervals of interest, τ_1 - τ_3 with a repeated-measures ANOVA. Stimulus ambiguity (LA, HA), time intervals (1, 2, 3), and EEG sensory region (O, P, Cp, C, Fc, F, Fp) were used as within-subject factors.

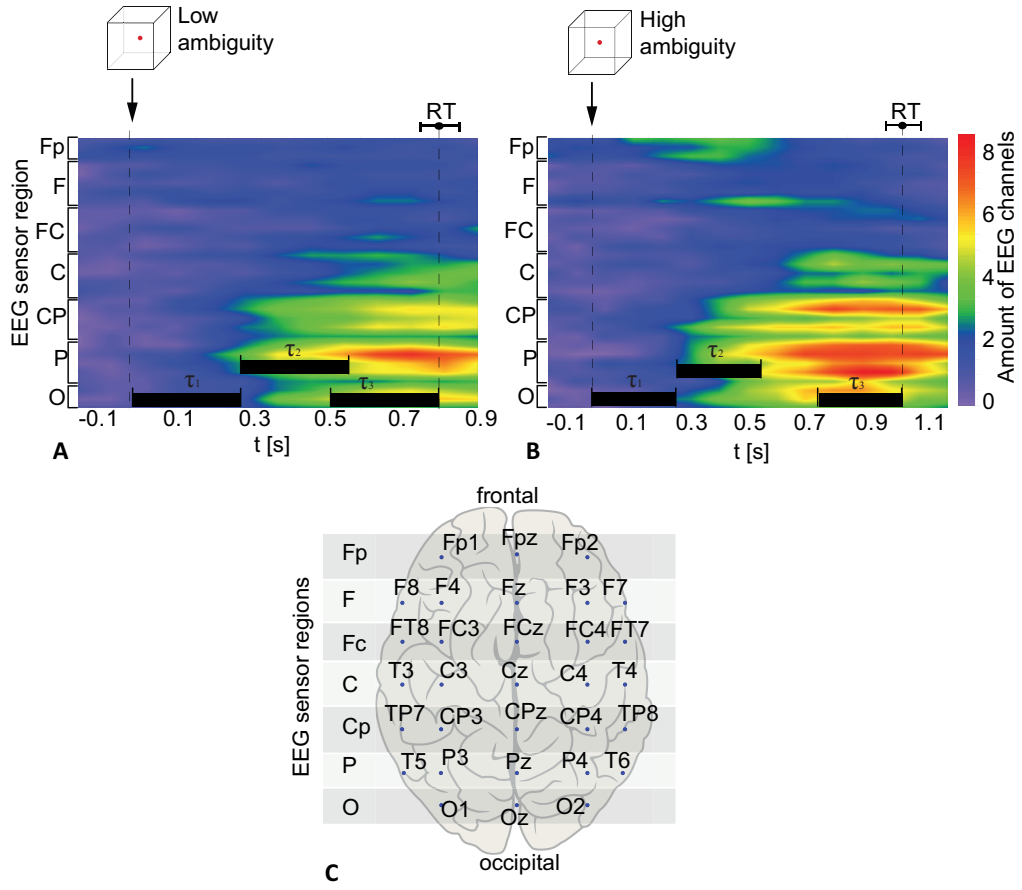

Figure 1. Distribution of the number of EEG channels exhibiting increase of the β-band spectral amplitude over the EEG sensor regions for the LA (A) and HA stimuli (B). (C) The 10-10 EEG sensors layout with 31 electrodes divided into seven EEG sensor regions: O, P, CP, C, Fc. F, Fp.

The repeated-measures ANOVA with the Greenhouse-Geisser correction showed an insignificant main effect of the ambiguity ($F_{1,19} = 2.518, p = 0.129$) and the EEG sensor regions ($F_{1.484,28,202} = 2.785, p = 0.092$). At the same time, we observed a significant main effect of the interval ($F_{1.084,20.6} = 8.395, p = 0.008$). Finally, there were significant interaction effects: time interval*EEG sensor area ($F_{2.38,45.226} = 11.072, p < 0.001$) and ambiguity*time interval*EEG sensor area ($F_{4.459,84.716} = 4.444, p = 0.002$), but the interactions ambiguity*time

Downloaded From: https://www.spiedigitallibrary.org/conference-proceedings-of-spie on 07 May 2021
Terms of Use: https://www.spiedigitallibrary.org/terms-of-use

interval ($F_{1.484,28.203} = 3.194, p = 0.69$) and ambiguity*EEG sensor area ($F_{2.398,45.559} = 1.188, p = 0.32$) were insignificant.

The observed interaction effect (ambiguity*time interval*EEG sensor region) suggested that N changed in a different way depending on the EEG sensor regions and the stimulus ambiguity. To find the spatio-temporal localization of the difference between the LA and HA stimuli, We contrasted the N-value between the time intervals for the different EEG sensor regions and the different ambiguity separately (Figure 2).

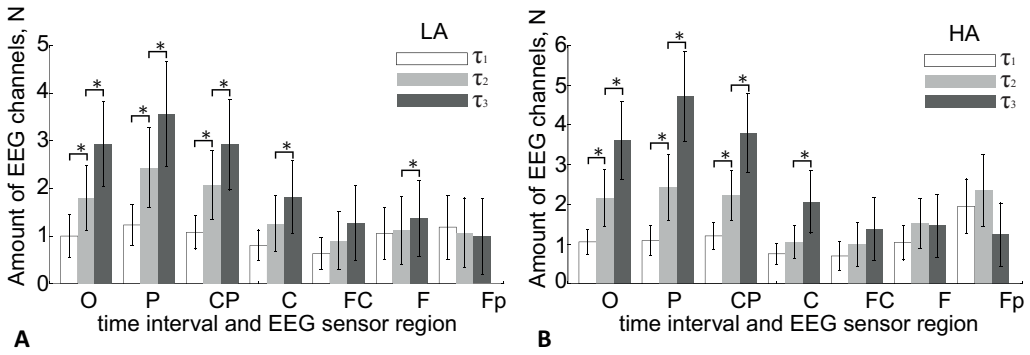

Figure 2. The number of EEG sensors N showing an increase in the spectral amplitude of the β-range compared to the time interval and area of EEG sensors for stimuli LA (A) and HA (B).

Region O: the paired samples t-test reveals that N significantly increases for τ_2 when compared with τ_1 for both LA ($\Delta N = 0.8 \pm 0.286\text{SE}, df = 19, t = 2.792, p = 0.012$) and HA ($\Delta N = 1.11 \pm 0.41\text{SE}, df = 19, t = 2.72, p = 0.014$) stimuli. The same is also observed for for τ_3 when compared with τ_2 for both LA ($\Delta N = 1.13 \pm 0.304\text{SE}, df = 19, t = 3.724, p = 0.001$) and HA ($\Delta N = 1.45 \pm 0.42\text{SE}, df = 19, t = 3.443, p = 0.003$) stimuli.

Region P: N significantly increases for τ_2 when compared with τ_1 for both LA ($\Delta N = 1.2 \pm 0.43\text{SE}, df = 19, t = 2.782, p = 0.012$) and HA ($\Delta N = 1.34 \pm 0.5\text{SE}, df = 19, t = 2.667, p = 0.015$) stimuli. The same is also observed for for τ_3 when compared with τ_2 for both LA ($\Delta N = 1.13 \pm 0.37\text{SE}, df = 19, t = 2.979, p = 0.008$) and HA ($\Delta N = 2.29 \pm 0.42\text{SE}, df = 19, t = 5.368, p < 0.001$) stimuli.

Region CP: N significantly increases for τ_2 when compared with τ_1 for both LA ($\Delta N = 0.99 \pm 0.38\text{SE}, df = 19, t = 2.547, p = 0.02$) and HA ($\Delta N = 1.02 \pm 0.36\text{SE}, df = 19, t = 2.775, p = 0.012$) stimuli. The same is also observed for for τ_3 when compared with τ_2 for both LA ($\Delta N = 0.85 \pm 0.29\text{SE}, df = 19, t = 2.842, p = 0.01$) and HA ($\Delta N = 1.57 \pm 0.38\text{SE}, df = 19, t = 4.11, p = 0.001$) stimuli.

Region C: N insignificantly changes for τ_2 when compared with τ_1 for both LA ($\Delta N = 0.45 \pm 0.27\text{SE}, df = 19, t = 1.633, p = 0.119$) and HA ($\Delta N = 0.3 \pm 0.21\text{SE}, df = 19, t = 1.377, p = 0.185$) stimuli. At the same time, the significant increase of N is observed for for τ_3 when compared with τ_2 for both LA ($\Delta N = 0.56 \pm 0.2\text{SE}, df = 19, t = 2.746, p = 0.013$) and HA ($\Delta N = 1.02 \pm 0.38\text{SE}, df = 19, t = 2.629, p = 0.017$) stimuli.

Region FC: N insignificantly changes for τ_2 when compared with τ_1 for both LA ($\Delta N = 0.27 \pm 0.29\text{SE}, df = 19, t = 0.912, p = 0.373$) and HA ($\Delta N = 0.29 \pm 0.24\text{SE}, df = 19, t = 1.161, p = 0.26$) stimuli. The same is observed for for τ_3 when compared with τ_2 for both LA ($\Delta N = 0.37 \pm 0.19\text{SE}, df = 19, t = 1.905, p = 0.072$) and HA ($\Delta N = 0.38 \pm 0.28\text{SE}, df = 19, t = 1.338, p = 0.197$) stimuli.

Region F: N changes in different way for LA and HA stimuli. For LA stimuli the paired samples t-test reveals that N does not change for τ_2 when compared with τ_1 ($\Delta N = 0.07 \pm 0.18\text{SE}, df = 19, t = 0.376, p = 0.711$) and significantly increases for τ_3 when compared with τ_2 ($\Delta N = 0.25 \pm 0.11\text{SE}, df = 19, t = 2.227, p = 0.038$). For HA stimuli N does not change for τ_2 when compared with τ_1 ($\Delta N = 0.48 \pm 0.23\text{SE}, df = 19, t = 2.086, p = 0.051$) as well as for τ_3 when compared with τ_2 ($\Delta N = -0.06 \pm 0.28\text{SE}, df = 19, t = -0.208, p = 0.837$).

Region Fp: N insignificantly changes for τ_2 when compared with τ_1 for both LA ($\Delta N = -0.11 \pm 0.13\text{SE}, df = 19, t = -0.863, p = 0.399$) and HA ($\Delta N = 0.4 \pm 0.29\text{SE}, df = 19, t = 1.357, p = 0.191$) stimuli. The same is

Downloaded From: https://www.spiedigitallibrary.org/conference-proceedings-of-spie on 07 May 2021
Terms of Use: https://www.spiedigitallibrary.org/terms-of-use

observed for for τ_3 when compared with τ_2 for both LA ($\Delta N = -0.083 \pm 0.148\text{SE}, df = 19, t = -0.560, p = 0.582$) and HA ($\Delta N = -1.11 \pm 0.62\text{SE}, df = 19, t = -1.793, p = 0.089$) stimuli.

4. CONCLUSION

We analyzed the spatial and temporal properties of the neural activity in the β-frequency band during the processing of ambiguous bistable stimuli. We tested how the stimulus ambiguity influenced the perceptual decision-making process. We found an increase in the number of EEG sensors (N_{inc}) that show an increase in the spectral amplitude with the visual stimulus's processing time. At the early sensory processing stages ($t < 0.3$ s), the stimuli with low and high ambiguity were characterized by the same N_{inc} distribution across the EEG sensor regions. This distribution had a local maximum in the frontal area.

For the decision-making stage (0.3 s before the response), the N_{inc} distributions had a local maximum in the parietal region. For the stimuli with a high degree of ambiguity, N_{inc} achieved higher values in the parietal and temporal areas.

Finally, for the $0.3 < t < 0.6$ s, processing of the stimuli with a high degree of ambiguity was characterized by the higher N_{inc} across the frontal EEG sensors. We supposed that processing the images with a low ambiguity was completed at this interval, but for the high ambiguity, it was still going. Moreover, it required more cognitive resources and activated frontal areas.

5. ACKNOWLEDGMENTS

This work has been supported by the Russian Science Foundation (project No 20-72-00036).

REFERENCES

[1] Milton, A. and Pleydell-Pearce, C. W., "The phase of pre-stimulus alpha oscillations influences the visual perception of stimulus timing," *Neuroimage* **133**, 53–61 (2016).

[2] Hramov, A. E., Frolov, N. S., Maksimenko, V. A., Makarov, V. V., Koronovskii, A. A., Garcia-Prieto, J., Antón-Toro, L. F., Maestú, F., and Pisarchik, A. N., "Artificial neural network detects human uncertainty," *Chaos: An Interdisciplinary Journal of Nonlinear Science* **28**(3), 033607 (2018).

[3] Pisarchik, A. N., Maksimenko, V. A., Andreev, A. V., Frolov, N. S., Makarov, V. V., Zhuravlev, M. O., Runnova, A. E., and Hramov, A. E., "Coherent resonance in the distributed cortical network during sensory information processing," *Scientific Reports* **9**(1), 1–9 (2019).

[4] Tanaka, M., Shigihara, Y., Ishii, A., Funakura, M., Kanai, E., and Watanabe, Y., "Effect of mental fatigue on the central nervous system: an electroencephalography study," *Behavioral and brain functions* **8**(1), 1–8 (2012).

[5] Maksimenko, V. A., Hramov, A. E., Frolov, N. S., Lüttjohann, A., Nedaivozov, V. O., Grubov, V. V., Runnova, A. E., Makarov, V. V., Kurths, J., and Pisarchik, A. N., "Increasing human performance by sharing cognitive load using brain-to-brain interface," *Frontiers in neuroscience* **12**, 949 (2018).

[6] Maksimenko, V. A., Runnova, A. E., Zhuravlev, M. O., Makarov, V. V., Nedayvozov, V., Grubov, V. V., Pchelintceva, S. V., Hramov, A. E., and Pisarchik, A. N., "Visual perception affected by motivation and alertness controlled by a noninvasive brain-computer interface," *PloS one* **12**(12), e0188700 (2017).

[7] Maksimenko, V. A., Hramov, A. E., Grubov, V. V., Nedaivozov, V. O., Makarov, V. V., and Pisarchik, A. N., "Nonlinear effect of biological feedback on brain attentional state," *Nonlinear Dynamics* **95**(3), 1923–1939 (2019).

[8] Maksimenko, V. A., Frolov, N. S., Hramov, A. E., RUNNOVA, A. E., Grubov, V. V., Kurths, J., and Pisarchik, A. N., "Neural interactions in a spatially-distributed cortical network during perceptual decision-making," *Frontiers in behavioral neuroscience* **13**, 220 (2019).

[9] Sehatpour, P., Molholm, S., Schwartz, T. H., Mahoney, J. R., Mehta, A. D., Javitt, D. C., Stanton, P. K., and Foxe, J. J., "A human intracranial study of long-range oscillatory coherence across a frontal–occipital–hippocampal brain network during visual object processing," *Proceedings of the National Academy of Sciences* **105**(11), 4399–4404 (2008).

Downloaded From: https://www.spiedigitallibrary.org/conference-proceedings-of-spie on 07 May 2021
Terms of Use: https://www.spiedigitallibrary.org/terms-of-use

[10] Chand, G. B. and Dhamala, M., "Interactions between the anterior cingulate-insula network and the fronto-parietal network during perceptual decision-making," *Neuroimage* **152**, 381–389 (2017).

[11] Kornmeier, J., Friedel, E., Wittmann, M., and Atmanspacher, H., "Eeg correlates of cognitive time scales in the necker-zeno model for bistable perception," *Consciousness and cognition* **53**, 136–150 (2017).

[12] Hramov, A. E., Maksimenko, V. A., Pchelintseva, S. V., Runnova, A. E., Grubov, V. V., Musatov, V. Y., Zhuravlev, M. O., Koronovskii, A. A., and Pisarchik, A. N., "Classifying the perceptual interpretations of a bistable image using eeg and artificial neural networks," *Frontiers in neuroscience* **11**, 674 (2017).

[13] Hramov, A. E., Maksimenko, V., Koronovskii, A., Runnova, A. E., Zhuravlev, M., Pisarchik, A. N., and Kurths, J., "Percept-related eeg classification using machine learning approach and features of functional brain connectivity," *Chaos: An Interdisciplinary Journal of Nonlinear Science* **29**(9), 093110 (2019).

[14] Pavlov, A. N., Hramov, A. E., Koronovskii, A. A., Sitnikova, E. Y., Makarov, V. A., and Ovchinnikov, A. A., "Wavelet analysis in neurodynamics," *Physics-Uspekhi* **55**(9), 845 (2012).

[15] Sitnikova, E., Hramov, A. E., Grubov, V., and Koronovsky, A. A., "Time-frequency characteristics and dynamics of sleep spindles in wag/rij rats with absence epilepsy," *Brain Research* **1543**, 290–299 (2014).

Downloaded From: https://www.spiedigitallibrary.org/conference-proceedings-of-spie on 07 May 2021
Terms of Use: https://www.spiedigitallibrary.org/terms-of-use